

# Conditions for the emergence of spatial asymmetric retrieval states in attractor neural network

Kostadin Koroutchev <sup>\*(1)</sup> and Elka Korutcheva <sup>†(2)</sup>

June 28, 2018

<sup>(1)</sup> Depto. de Ingeniería Informática  
Universidad Autónoma de Madrid, 28049 Madrid, Spain

<sup>(2)</sup> Depto. de Física Fundamental,  
Universidad Nacional de Educación a Distancia,  
c/Senda del Rey, No 9, 28080 Madrid, Spain

## Abstract

In this paper we show that during the retrieval process in a binary symmetric Hebb neural network, spatial localized states can be observed when the connectivity of the network is distance-dependent and constraint on the activity of the network is imposed, which forces different level of activity in the retrieval and learning states. This asymmetry in the activity during the retrieval and learning is found to be sufficient condition in order to observe spatial localized retrieval states. The result is confirmed analytically and by simulation. **Keywords:** neural networks, spatial localized states, replica formalism  
**PACS:** 64.60.Cn, 84.35.+i, 89.75.-k, 89.75.Fb

---

<sup>\*</sup>Corresponding author; k.koroutchev@uam.es; Inst. for Computer Systems, Bulgarian Academy of Sciences, 1113, Sofia, Bulgaria

<sup>†</sup>G.Nadjakov Institute of Solid State Physics, Bulgarian Academy of Sciences, 1784, Sofia, Bulgaria

# 1 Introduction

In a recent publication [1] it was shown that using linear-threshold model neurons, Hebb learning rule, sparse coding and distance-dependent asymmetric connectivity, spatial asymmetric retrieval states (SAS) can be observed. This asymmetric states are characterized by a spatial localization of the activity of the neurons, described by the formation of local bumps.

Similar results have been reported in the case of Hebb binary model for associative neural network [2]. The observation is intriguing, because all components of the network are intrinsically symmetric with respect to the positions of the neurons and the retrieved state is clearly asymmetric. An illustration of SAS in binary network is presented in Fig.3.

In parallel to the present investigation, extensive computer simulations have been performed in the case of integrate and fire neurons [3], where bump formations were also reported. These results are in agreement with our previous results [2] that networks of binary neurons do not show bumpy retrieval solutions when the stored and retrieved patterns have the same mean activity.

The biological reason for this phenomenon is based on the transient synchrony that leads to recruitment of cells into local bumps, followed by desynchronized activity within the group [4],[5].

When the network is sufficiently diluted, say less than 5%, then the differences between asymmetric and symmetric connectivity are minimal [6]. For this reason we expect that the impact of the asymmetrical connectivity will be minimal and the asymmetry could not be considered as necessary condition for the existence of SAS, as it is confirmed in the present work.

There are several factors that possibly contribute to the SAS in model network.

In order to introduce the spatial effects in neural networks(NN), one essentially needs distance measures and topology between the neurons, imposing some distribution on the connections, dependent on that topology and distances. The major factor to observe spatial asymmetric activity is of course the spatially dependent connectivity of the network. Actually this is an essential condition, because given a network with SAS, by applying random permutation to the enumeration of the neurons, one will obviously achieve states without SAS. Therefore, the topology of the connections must depend on the

distance between the neurons.

Due to these arguments, a symmetric and distance-dependent connectivity for all neurons is chosen in this study.

We consider an attractor NN model of Hebbian type formed by  $N$  binary neurons  $\{S_i\}, S_i \in \{-1, 1\}, i = 1, \dots, N$ , storing  $p$  binary patterns  $\xi_i^\mu, \mu \in \{1 \dots p\}$ , and we assume a symmetric connectivity between the neurons  $c_{ij} = c_{ji} \in \{0, 1\}, c_{ii} = 0$ .  $c_{ij} = 1$  means that neurons  $i$  and  $j$  are connected. We regard only connectivities in which the fluctuations between the individual connectivity are small, e.g.  $\forall_i \sum_j c_{ij} \approx cN$ , where  $c$  is the mean connectivity.

The learned patterns are drawn from the following distribution:

$$P(\xi_i^\mu) = \frac{1+a}{2} \delta(\xi_i^\mu - 1 + a) + \frac{1-a}{2} \delta(\xi_i^\mu + 1 + a),$$

where the parameter  $a$  is the sparsity of the code. Note that the notation is a little bit different from the usual one. By changing the variables  $\eta \rightarrow \xi + a$  and substituting in the above equation, one obtains the usual form for the pattern distribution in the case of sparse code [7].

Further in this article we show that imposing symmetry between the retrieval and the learning states, i.e. equal probability distributions of the patterns and the network activities, no SAS exists. Spatial asymmetry can be observed only when asymmetry between the learning and the retrieval states is imposed.

Actually, by using binary network and symmetrically distributed patterns, the only asymmetry between the retrieval and the learning states that can be imposed, independent on the position of the neurons, is the total number of the neurons in a given state. Having in mind that there are only two possible states, this condition leads to a condition on the mean activity of the network.

To impose a condition on the mean activity, we add an extra term  $H_a$  to the Hamiltonian

$$H_a = NR \sum_i S_i / N.$$

This term actually favors states with lower total activity  $\sum_i S_i$  that is equivalent to decrease the number of active neurons, creating asymmetry between the learning and the retrieval states. If the value of the parameter  $R = 0$ , the corresponding model has been intensively studied since the classical results of Amit et al. [8] for symmetrical

code and Tsodyks, Feigel'man [7] for sparse code. These results show that the sparsities of the learned patterns and the retrieval states are the same and equal to  $aN$ . In the case  $R \neq 0$ , the energy of the system increases with the number of active neurons ( $S_i = 1$ ) and the term  $H_a$  tends to limit the number of active neurons below  $aN$ . Roughly speaking, the parameter  $R$  can be interpreted as some kind of chemical potential for the system to force a neuron in a state  $S = 1$ . Here we would like to mention that Roudi and Treves [1] have also stated that the activity of the linear-threshold network, they study, has to be constrained in order to have spatially asymmetric states. However, no explicit analysis was presented in order to explain the phenomenon and the condition is not shown to be sufficient one, probably because the use of more complicated linear threshold neurons diminishes the importance of this condition. Here we point out the importance of the constraint on the network level of activity and show that it is a sufficient condition for observation of spatial asymmetric states in binary Hebb neural network.

The goal of this article is to find minimal necessary conditions where SAS can be observed. We start with general sparse code and sparse distance-dependent connectivity and using replica symmetry paradigm we find the equations for the order parameters.

Then we study the solutions of these equations using some approximations and compare the analytical results with simulation.

The conclusion, drawn in the last part, shows that only the asymmetry between the learning and the retrieval states is sufficient to observe SAS.

## 2 Analytical analysis

### 2.1 Connectivity matrix

For the analytical analysis of the SAS states, we consider the decomposition of the connectivity matrix  $c_{ij}$  by its eigenvectors  $a_i^{(k)}$ :

$$c_{ij} = \sum_k \lambda_k a_i^{(k)} a_j^{(k)}, \quad \sum_i a_i^{(k)} a_i^{(l)} = \delta_{kl}, \quad (1)$$

where  $\lambda_k$  are the corresponding (positive) eigenvalues. The eigenvectors  $a_i^{(k)}$  are ordered by its corresponding eigenvalues in decreasing order, e.g.

$$\forall a_j^{(k)}, a_j^{(l)}, k > l \Rightarrow \lambda_k \leq \lambda_l. \quad (2)$$

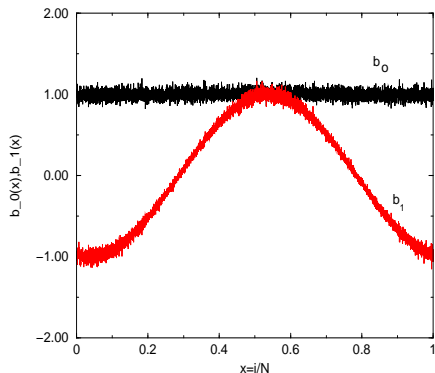


Figure 1: The components of the first eigenvectors of the connectivity matrix, normalized by a square root of their corresponding eigenvalue, in order to eliminate the effect of the size of the network. The first eigenvector has a constant component, the second one sine-like component.  $N = 6400$ ,  $c = 320/N$ ,  $\lambda_0 = 319.8$ ,  $\lambda_1 = 285.4$ .

For convenience we introduce also the parameters  $b_i^k$ :

$$b_i^k \equiv a_i^{(k)} \sqrt{\lambda_k/c}. \quad (3)$$

To get some intuition of what  $a_j^{(k)}$  look like, we plot in Fig. 1 the first two eigenvectors  $a^0$  and  $a^1$ .

For a wide variety of connectivities, the first three eigenvectors are approximately the following:

$$a_k^{(0)} = \sqrt{1/N}, \quad a_k^{(1)} = \sqrt{2/N} \cos(2\pi k/N), \quad a_k^{(2)} = \sqrt{2/N} \sin(2\pi k/N). \quad (4)$$

Further, the eigenvalue  $\lambda_0$  is approximately the mean connectivity of the network per node, that is the mean number of connections per neuron  $\lambda_0 = cN$ .

## 2.2 Hamiltonian

Following the classical analysis of Amit et al. [8], we study binary Hopfield model [9]

$$H_{int} = -\frac{1}{cN} \sum_{ij\mu} S_i \xi_i^\mu c_{ij} \xi_j^\mu S_j, \quad (5)$$

where the matrix  $c_{ij}$  denotes the matrix of connectivity and we have assumed Hebb's rule of learning [10].

In order to take into account the finite numbers of overlaps that condense macroscopically, we use Bogolyubov's method of quasi averages [11]. To this aim we introduce an external field, conjugate to a final number of patterns  $\{\xi_i^\nu\}, \nu = 1, 2, \dots, s$  by adding a term

$$H_h = - \sum_{\nu=1}^s h^\nu \sum_i \xi_i^\nu S_i \quad (6)$$

to the Hamiltonian.

Finally, as we already mentioned in the Introduction, in order to impose some asymmetry in the neural network's states, we also add the term

$$H_a = NR \left( \frac{1}{N} \sum_i S_i \right) \approx NR \overline{S_i b_i^0}, \quad (7)$$

where we used  $b_i^0 \approx 1$ . The equality is exact for equal degree network. The over line in eq.(7) means spatial averaging:  $\overline{(\cdot)} = \frac{1}{N} \sum_i (\cdot)$ .

The whole Hamiltonian we are studying now is  $H = H_{int} + H_h + H_a$ :

$$H = - \frac{1}{cN} \sum_{ij\mu} S_i \xi_i^\mu c_{ij} \xi_j^\mu S_j - \sum_{\nu=1}^s h^\nu \sum_i \xi_i^\nu S_i + NR \overline{S_i b_i^0}. \quad (8)$$

## 2.3 RS solution

By using the "replica formalism" [12], for the averaged free energy per neuron we get:

$$f = \lim_{n \rightarrow 0} \lim_{N \rightarrow \infty} \frac{-1}{\beta n N} (\langle \langle Z^n \rangle \rangle - 1), \quad (9)$$

where  $\langle \langle \dots \rangle \rangle$  stands for the average over the pattern distribution  $P(\xi_i^\mu)$ ,  $n$  is the number of the replicas, which are later taken to zero and  $\beta$  is the inverse temperature.

Following [8], [13], the replicated partition function is represented by decoupling the sites using an expansion of the connectivity matrix  $c_{ij}$  over its eigenvalues  $\lambda_l, l = 1, \dots, M$  and eigenvectors  $a_i^l$  (eq.1):

$$\begin{aligned} \langle \langle Z^n \rangle \rangle = e^{-\beta \alpha N n / 2c} \left\langle \left\langle \text{Tr}_{S^\rho} \exp \left[ \frac{\beta}{2N} \sum_{\mu\rho l} \sum_{ij} (\xi_i^\mu S_i^\rho b_i^l) (\xi_j^\mu S_j^\rho b_j^l) + \right. \right. \right. \\ \left. \left. \left. \beta \sum_{\nu} h^\nu \sum_{i\rho} \xi_i^\nu S_i^\rho - \beta RN \sum_{i\rho} b_i^0 S_i^\rho / N \right] \right\rangle \right\rangle, \quad (10) \end{aligned}$$

with  $\alpha = p/N$  being the storage capacity.

Following the classical approach of Amit et al.[8] we introduce variables  $m_{\rho k}^\mu$  for each replica  $\rho$  and each eigenvalue and split the sums over the first  $s$  “condensed” patterns, labeled by the letter  $\nu$  and the remaining (infinite)  $p - s$ , over which an average and a later expansion over their corresponding parameters was done.<sup>1</sup> We have supposed that only a finite number of  $m_k^\nu$  are of order one and those are related to the largest eigenvalues  $\lambda_k$ .

As a next step, we introduce the order parameters (OP)

$$q_k^{\rho,\sigma} = \overline{(b_i^k)^2 S_i^\rho S_i^\sigma},$$

where  $\rho, \sigma = 1, \dots, n$  label the replica indexes. Note the role of the connectivity matrix on the OP  $q_k^{\rho,\sigma}$  by the introduction of the parameters  $b_i^k$ .

The introduction of the OP  $r_k^{\rho,\sigma}$ , conjugate to  $q_k^{\rho,\sigma}$ , and the use of the replica symmetry ansatz [12]  $m_{\rho k}^\nu = m_k^\nu, q_k^{\rho,\sigma} = q_k$  for  $\rho \neq \sigma$  and  $r_k^{\rho,\sigma} = r_k$  for  $\rho \neq \sigma$ , followed by a suitable linearization of the quadratic in  $S$ -terms and the application of the saddle-point method [8], give the following final form for the free energy per neuron:

$$\begin{aligned} f &= \frac{1}{2c} \alpha (1 - a^2) + \frac{1}{2} \sum_k (m_k)^2 - \frac{\alpha \beta (1 - a^2)}{2} \sum_k r_k q_k + \frac{\alpha \beta (1 - a^2)}{2} \sum_k \mu_k r_k + \\ &+ \frac{\alpha}{2\beta} \sum_k [\ln(1 - \beta(1 - a^2)\mu_k + \beta(1 - a^2)q_k) - \\ &- \beta(1 - a^2)q_k(1 - \beta(1 - a^2)\mu_k + \beta(1 - a^2)q_k)^{-1}] - \\ &- \frac{1}{\beta} \int \frac{dz e^{-\frac{z^2}{2}}}{\sqrt{2\pi}} \ln 2 \cosh \beta \left( z \sqrt{\alpha(1 - a^2) \sum_l r_l b_i^l b_i^l + \sum_l m_l \xi_i b_i^l + R b_i^0} \right). \end{aligned} \quad (11)$$

In the last expression we have introduced the variables  $\mu_k = \lambda_k/cN$  and we have used the fact that the average over a finite number of patterns  $\xi^\nu$  can be self-averaged [8]. In our case however the self-averaging is more complicated in order to preserve the spatial dependence of the retrieved pattern. The detailed analysis will be given in a forthcoming publication [14].

---

<sup>1</sup>Without loss of generality we can limit ourself to the case of only one pattern with macroscopic overlap ( $\nu = 1$ ). The generalization to  $\nu > 1$  is straightforward.

The equations for the OP  $r_k$ ,  $m_k$  and  $q_k$  are respectively:

$$r_k = \frac{q_k(1-a^2)}{(1-\beta(1-a^2)(\mu_k - q_k))^2}, \quad (12)$$

$$m_k = \int \frac{dz e^{-\frac{z^2}{2}}}{\sqrt{2\pi}} \xi_i b_i^k \tanh \beta \left( z \sqrt{\alpha(1-a^2) \sum_l r_l b_i^l b_i^l + \sum_l m_l \xi_i b_i^l + R b_i^0} \right) \quad (13)$$

and

$$q_k = \int \frac{dz e^{-\frac{z^2}{2}}}{\sqrt{2\pi}} (b_i^k)^2 \tanh^2 \beta \left( z \sqrt{\alpha(1-a^2) \sum_l r_l b_i^l b_i^l + \sum_l m_l \xi_i b_i^l + R b_i^0} \right). \quad (14)$$

At  $T = 0$ , keeping  $C_k \equiv \beta(\mu_k - q_k)$  finite and limiting the above system only to the first two coefficients, the above equations read:

$$m_0 = \frac{1-a^2}{4\pi} \int_{-\pi}^{\pi} g(\phi) d\phi \quad (15)$$

$$m_1 = \sqrt{2\mu_1} \frac{1-a^2}{4\pi} \int_{-\pi}^{\pi} g(\phi) \sin \phi d\phi \quad (16)$$

$$C_0 = \frac{1}{2\pi} \int_{-\pi}^{\pi} g_c(\phi) d\phi \quad (17)$$

$$C_1 = \frac{\mu_1}{\pi} \int_{-\pi}^{\pi} g_c(\phi) \sin^2 \phi d\phi \quad (18)$$

$$r_k = \frac{\mu_k(1-a^2)}{[1-(1-a^2)C_k]^2}, \quad (19)$$

where

$$g(\phi) = \operatorname{erf}(x_1) + \operatorname{erf}(x_2) \quad (20)$$

$$g_c(\phi) = [(1+a)e^{-(x_1)^2} + (1-a)e^{-(x_2)^2}]/[\sqrt{\pi}y] \quad (21)$$

$$x_1 = [(1-a)(m_0 + m_1 \sqrt{2\mu_1} \sin \phi) + R]/y \quad (22)$$

$$x_2 = [(1+a)(m_0 + m_1 \sqrt{2\mu_1} \sin \phi) - R]/y \quad (23)$$

$$y = \sqrt{2\alpha(1-a^2)(r_0 + 2\mu_1 r_1 \sin^2 \phi)}. \quad (24)$$

When we assume  $m_1 = m_2 = \dots = 0, R = 0$ , we obtain the result of Gardner [13]. When additionally  $\mu_1 = 0$  we obtain the result of Amit et al. [8]. Of course, in this approximation no conclusion about



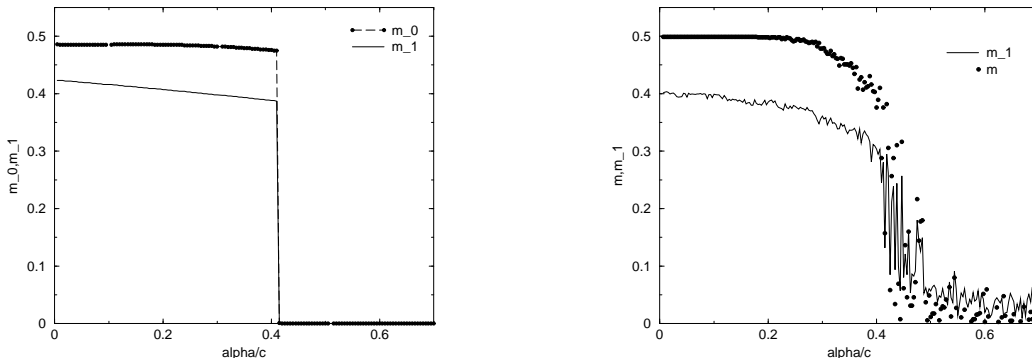


Figure 2: Left – Computation of  $m_0, m_1$  according to the eqs.(15-19). The sparsity of the code is  $a = 0.2$  and  $R = 0.57$ . The sharp bound is due to the limitation of the equations only to the first two terms of the OP  $m, r, C$ , as well as to the finite scale effects. The result of the simulations is represented on the right side.

the size of the bump can be drawn, because the bump characteristic size is fixed to the characteristic size of a sine wave, that is always one half of the size of the network.

The result of the numerical solution of the eqs.(15-19) is show in Fig. 2 (left). The sharp bound of the phase transition is a result of taking into account just two terms  $k = 0, 1$  and the lack of finite-size effects in the thermodynamic limit.

### 3 Simulations

In order to compare the results, we also performed computer simulations. To this aim we chose the network's topology to be a circular ring, with a distance measure

$$|i - j| \equiv \min(i - j + N \bmod N, j - i + N \bmod N)$$

and used the same connectivity as in Ref.[1] with typical connectivity distance  $\sigma_x N$ :

$$P(c_{ij} = 1) = c \left[ \frac{1}{\sqrt{2\pi}\sigma_x N} e^{-(|i-j|/N)^2/2\sigma_x^2} + p_0 \right].$$

Here the parameter  $p_0$  is chosen to normalize the expression in the brackets. When  $\sigma_x$  is small enough, then spatial asymmetry is expected.

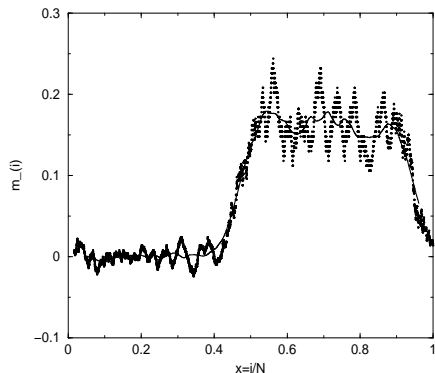


Figure 3: Typical bump form. The figure shows the running average of the local overlap  $m_{(i)} = S_i \xi_i$  vs the position of the neuron (run length 100 and 300). The sparsity of the code is  $a = 0.2$ ,  $R$  is chosen to supply 0.5 of the unconstrained activity.  $N = 6400, c = 0.05$ .

In order to measure the overlap between the states of the patterns and the neurons and the effect of the single-bump spatial activity during the simulation, we used the ratio  $m_1/m_0$ , where

$$m_0 = \frac{1}{N} \sum_k \xi_k^0 S_k$$

and

$$m_1 = \frac{1}{N} \left| \sum_k \xi_k^0 S_k e^{2\pi i k/N} \right|.$$

Because the sine waves appear first,  $m_1/m_0$  results also to be a sensitive asymmetric measure, at least compared to the visual inspection of the running averages of the local overlap  $m_{(i)} \equiv \xi_i S_i$ . An example of the local overlap form is given in Fig.3.

Let us note that  $m_1$  can be regarded as the power of the first Fourier component and  $m_0$  can be regarded as a zeroth Fourier component, that is the power of the direct-current component.

The corresponding behavior of the order parameters  $m_0, m_1$  in the zero-temperature case, obtained by the simulations, is represented in Fig. 2 (right). Note the good correspondence between the numerical solution of the analytical results and the results obtained by simulation.

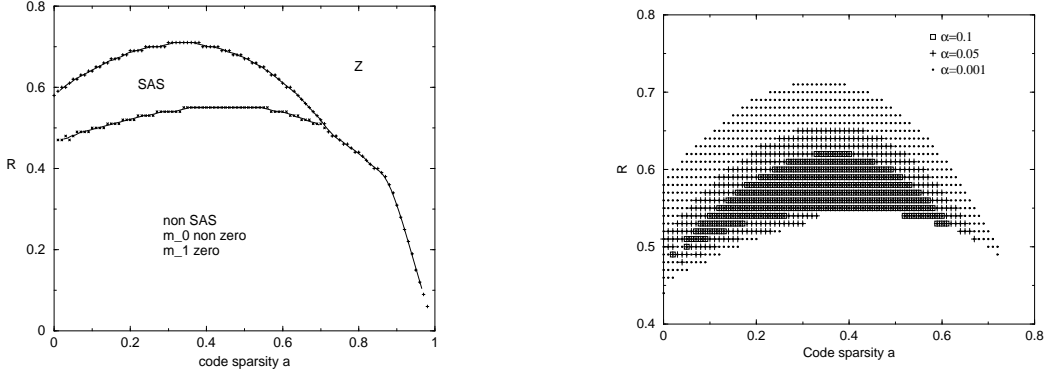


Figure 4: Left: Phase diagram  $R$  versus  $a$  for  $\alpha = 0.001$  ( $\alpha/c = 0.02$ ). The SAS region, where local bumps are observed is relatively large. The Z region corresponds to trivial solutions for the overlap. Right: SAS region for different values of  $\alpha$ . High values of  $\alpha$  limit the SAS region. Note that not all of the values of  $\alpha$  are feasible with arbitrary sparsity of the network  $c$ .

## 4 Discussion

We have investigated the phase diagram when fixing the capacity taking into account the connectivity of the network. We have observed a stable area of solutions corresponding to the formation of local bumps, i.e. solutions with OP  $m_1 \neq 0$  for wide range of the parameters load  $\alpha$ , sparsity  $a$  and the retrieval asymmetry parameter  $R$  (Fig.4). Note that  $\alpha = p/N$  that is used in this paper, although natural when working with eigenvectors, is slightly different from the usual one  $\alpha' = P/(cN) = \alpha/c$ . The range of values of  $\alpha/c$  corresponds to biologically plausible values.

According to this phase diagram, there exist states with  $a = 0$  and spatial asymmetric retrieval states. Therefore, the sparsity of the code is not a necessary condition for SAS. Also it is clear that there is no necessity to use more complex model neuron than a binary one in order to observe SAS. It is worth mention that the sparsity of the code makes SAS better pronounced.

On the other hand, there is no state with SAS and  $H_a = 0$ , and therefore the asymmetry between the retrieval activity and the learned patterns is essential for the observation of the phenomenon.

The diagram in Fig.4 shows a clear phase transition with  $R$ . For small values of  $R$ , the effect (SAS) is not present. If  $R > 1$ , then the

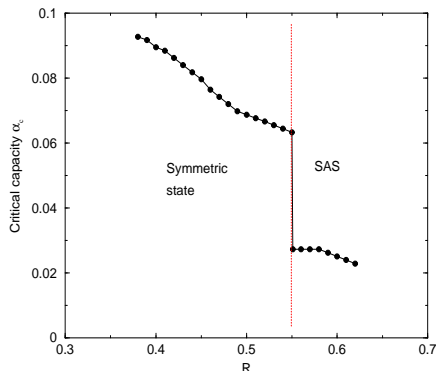


Figure 5: The critical storage capacity  $\alpha_c$  as a function of  $R$ .  $a = 0.4$  The drop of  $\alpha_c$  is clearly seen on the transition to SAS state.

only stable state is the trivial  $Z$  state, as all the nonzero solutions are suppressed. Only for intermediate values of  $R$ , the bumpiness occurs. The load  $\alpha$  of the network shrinks the area of parameters where bumps are observed. However, the area remains large enough for all values of  $\alpha$ .

Our observations show that the parameter  $R$  is a very rigid one in the sense that the behavior of the system changes drastically for small changes of  $R$ . Richer behavior can be obtained when the term  $H_a$  is replaced by a quadratic term of the total activity. Detailed analysis will be presented in a forthcoming publication [14].

When the network changes its behavior from homogeneous retrieval to spatial localized state, the critical storage capacity of the network drops dramatically, because effectively only the fraction of the network in the bump can be excited and the storage capacity drops proportionally to the size of the bump, Fig.5. As can be seen in this figure, in the phase transition point the capacity drops approximately twofold.

The local overlap of the bump remains strong but, in contrast to the linear threshold network, for binary neurons is always less than one. However, if the threshold is determined as a function of the distribution of the internal neuronal fields, as in [1], the impact on the storage capacity of the binary network near the transition points is minor, as it can be seen by simulations.

These effects are interesting and deserves more attention in the future.

## 5 Conclusion

In this paper we have studied the conditions for the appearance of spatial dependent activity in a binary neural network model.

The analysis was done analytically, which was possible due to the finite number of relevant order parameters, and is compared with simulations. The analytical approach gives a closed form for the equations describing the different order parameters and permits their analysis.

It was shown that the presence of the term  $H_a$  is sufficient for the existence of the SAS. Nor asymmetry of the connection, neither sparsity of the code are necessary to achieve spatial asymmetric states (bumps). In our opinion, this is the main result of the paper.

The numerical solution of the analytical results, as well as the simulations show that when  $H_a = 0$  no SAS can be observed. This is a good, although not conclusive argument, that the asymmetry between the retrieval and the learning states might be a necessary and not only sufficient condition for the observation of spatial asymmetry states.

Detailed analysis of the problem will be presented in a forthcoming publication.

## Acknowledgments

The authors thank A.Treves and Y.Roudi for stimulating discussions.

This work is financial supported by the Abdus Salam Center for Theoretical Physics, Trieste, Italy and by Spanish Grants CICYT, TIC 01-572, DGI.M.CyT.BFM2001-291-C02-01 and the program “Promoción de la Investigación UNED’02”.

## References

- [1] Y.Roudi and A.Treves, “An associate network with spatially organized connectivity” , *JSTAT* (2004) P07010, pp. 1-25.

- [2] K.Koroutchev and E.Korutcheva, “Spatial asymmetric retrieval states in symmetric Hebb network with uniform connectivity”, *Preprint ICTP*, Trieste, Italy, IC/2004/91, (2004), pp. 1-12.
- [3] A.Anishchenko, E.Bienenstock and A.Treves, *Autoassociative Memory Retrieval and Spontaneous Activity Bumps in Small-World Networks of Integrate-and-Fire Neurons*, Los Alamos, 2005, <http://xxx.lanl.gov/abs/q-bio.NC/0502003>.
- [4] J.Rubin and A.Bose, “Localized activity in excitatory neuronal networks”, *Network: Comput.Neural Syst.*, vol.15,(2004), pp. 133-158.
- [5] N.Brunel, “Dynamics and plasticity of stimulus-selective persistent activity in cortical network models”, *Cereb.Cortex*, vol.13,(2003),pp.1151-1161.
- [6] J. Hertz, A. Krogh and R. G. Palmer, *Introduction to the theory of neural computation*, Perseus Publishing Group, Santa Fe, 1991.
- [7] M.Tsodyks and M.Feigel'man, “Enhanced storage capacity in neural networks with low activity level”, *Europhys.Lett.*, vol.6,(1988), pp. 101-105.
- [8] D.Amit, H.Gutfreund and H.Sompolinsky, “Statistical mechanics of neural networks near saturation”,*Ann.Phys.*, vol.173,(1987),pp.30-67.
- [9] J.Hopfield, “Neural networks and physical systems with emergent collective computational abilities”, *Proc.Natl.Acad.Sci.USA*, vol.79,(1982), pp. 2554-2558.
- [10] D.Hebb, *The Organization of Behavior: A Neurophysiological Theory*, Wiley, New York, 1949.
- [11] N.N.Bogolyubov, *Physica(Suppl.)*, vol.26,(1960), S1.
- [12] M.Mézard, G.Parisi and M.-A.Virasoro, *Spin-glass theory and beyond*, World Scientific, Singapore, 1987.
- [13] A.Canning and E.Gardner, “Partially connected models of neural networks”, *J.Phys.A:Math.Gen.*, vol.21,(1988),pp.3275-3284.
- [14] K.Koroutchev and E.Korutcheva, in preparation.